Temperature influences on network formation of low DE maltodextrin gels

Kanyuck, Kelsey; Mills, Tom; Norton, Ian; Norton-Welch, Abigail

DOI:
10.1016/j.carbpol.2019.04.039

Document Version
Peer reviewed version

Citation for published version (Harvard):
Kanyuck, K, Mills, T, Norton, I & Norton-Welch, A 2019, 'Temperature influences on network formation of low DE maltodextrin gels', *Carbohydrate Polymers*, vol. 218, pp. 170-178. https://doi.org/10.1016/j.carbpol.2019.04.039

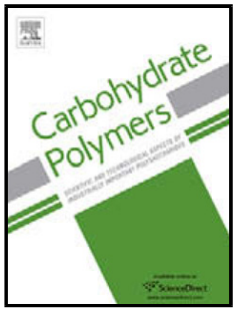

Title: Temperature influences on network formation of low DE maltodextrin gels

Authors: K.M. Kanyuck, T.B. Mills, I.T. Norton, A.B. Norton-Welch

PII: S0144-8617(19)30423-0
DOI: https://doi.org/10.1016/j.carbpol.2019.04.039
Reference: CARP 14813

To appear in:

Received date: 31 January 2019
Revised date: 5 April 2019
Accepted date: 8 April 2019

Please cite this article as: Kanyuck KM, Mills TB, Norton IT, Norton-Welch AB, Temperature influences on network formation of low DE maltodextrin gels, *Carbohydrate Polymers* (2019), https://doi.org/10.1016/j.carbpol.2019.04.039

Temperature influences on network formation of low DE maltodextrin gels

K. M. Kanyuck, T. B. Mills, I. T. Norton, A. B. Norton-Welch

School of Chemical Engineering, University of Birmingham, Edgbaston, Birmingham, B15 2TT, UK

*Contact information for the corresponding author: Kelsey Kanyuck. Tel: +44 121 414 5364 Email: KXK720@student.bham.ac.uk

Highlights

- Aggregation network varied in both degree and type with gelling temperature
- Lower temperatures created a stronger and crumbly gel
- Stronger gels corresponded to a network of greater enthalpy and entropy
- Bonds showed partial thermal irreversibility

Abstract

Gelation of maltodextrin (DE 2) was examined over a range of temperatures to understand the behaviour within mixed-gel systems. Maltodextrin solutions were prepared at 95° C and held at temperatures between 5°C and 60 °C for four days. Bulk gel properties and the underlying microstructure were analysed using fracture strength, proton relaxation time, and differential scanning calorimetry (DSC). Holding at lower temperatures led to a greater gel strength with a brittle and crumbly texture. Analysis of the microstructure showed that gelation at 10°C versus 60 °C produced a greater number of aggregates (melting enthalpy 14.5 J/g to 3.4 J/g) and structuring of a higher melting entropy (45 mJ/g·K to 10 mJ/g·K). A thermal hysteresis with signs of structure corresponding to both holding temperatures was also measured. Elevated temperature was hypothesized to decrease the amount of smaller molecular weight chains participating in aggregation by shifting from the helix to coil form.

Keywords

Maltodextrin; Helix–coil transition; Thermal Hysteresis; Differential Scanning Calorimetry; NMR

1. Introduction:

Maltodextrin is a widely used polymer in the food industry for applications including thickening, bulking, and encapsulation (Chronakis, 1998). Gelation of maltodextrin occurs at relatively high concentrations (10 to 20%) through association of double helix chains, with longer chains connecting aggregates to form the continuous network (Loret, Meunier, Frith, & Fryer, 2004; Reuther et al., 1984; Schierbaum, Reuther, Braudo, Plashchina, & Tolstoguzov, 1990). Higher concentrations lead to stronger and more solid gels with fracture properties of a brittle gel, but low concentrations have shown creamy appearances (Loret, Frith, & Fryer, 2004; Loret et al., 2004; Schierbaum et al., 1992). A handful of researchers have studied material properties of single maltodextrin systems and reported properties characteristic of physical gels (Bulpin, Cutler, & Dea, 1984; Kasapis, Morris, Norton, & Clark, 1993a; Loret et al., 2004; Loret et al., 2004; Schierbaum et al., 1992). When included in a mixed gel system, unique fat-like properties have been observed (Chronakis, 1998). Surrounding this effect, many studies have focused on maltodextrin mixed gels with gelatin (Brown, Foster, Norton, & Underdown, 1995; Butler & Heppenstall-Butler, 2003; Kasapis, Morris, Norton, & Brown, 1993; Kasapis, Morris, Norton, & Clark, 1993b; Lorn & Hermansson, 2000; Lundin et al., 2000; Nickerson et al., 2006; Normand, Plucknett, Pomfret, Ferdinando, & Norton, 2001), pectin (Picout, Richardson, & Morris, 2000), and agarose (Loret, Frith, & Fryer, 2006). Several patents have even been granted utilizing the unique creaminess of maltodextrin-gelatin mixed gel system for reduced fat food products (Cain et al., 1990; Wesdorp, Madsen, Norton, & Brown, 1995). From the findings of both single and mixed systems, gelling temperature and time were highlighted as key parameters in determining the maltodextrin gel properties.

Kinetics of gelation and the resulting microstructure have been impacted by holding time and temperature of the maltodextrin dispersion during gelation. An increasing gel strength (for up to 12 days) after initial formation is typically observed for maltodextrin (Chronakis & Kasapis, 1995; Loret et al., 2004). Both higher concentration and lower holding temperature increased the gelling rate, and the lowest temperatures formed the most solid gels (Schierbaum et al., 1992). Other studies have found that cooling rate and gel temperature impacted the rate of gel formation, but had a minimal impact on final gel strength (Loret et al., 2004; Loret et al., 2004). However, it is likely the range of temperatures examined (only up to 40 °C) and short time length (only up to 27 hours) reduced the potential for detecting differences. A general understanding of the initial gelling parameters has been established from these articles, but not yet an analysis of the material properties of an equilibrated gel. Expansion of the range of temperatures or gelation time would allow for a better understanding of network development of maltodextrin gels.

This article will compare maltodextrin network formations at a range of gelling temperatures. Previous articles have noted differences in gelation caused by temperature, however these experiments focused on rates of gelation rather than the equilibrated gel characterization (Kasapis et al., 1993a; Loret et al., 2004; Schierbaum et al., 1992). A strengthening of up to 14 days has been observed for maltodextrin gels (Chronakis & Kasapis, 1995; Loret et al., 2004), so the previous work has limited application to a final gel structure. Specifically, the maximum experimental time lengths were 13 hours (Loret et al., 2004), 40 minutes (Schierbaum et al., 1990), and 7 hours (Kasapis et al., 1993a). These short times have suggested a preliminary understanding but are unable to predict crystallization or structure development on an industry-relevant timescale. This work aims to provide a detailed characterization of the equilibrated microstructure to comprehensively assess how temperature influences network development. Additionally, even within the previously mentioned short time-scales, Schierbaum (1992) reported a partial thermal irreversibility in maltodextrin gels. Different solid-liquid ratios were observed for gels consistently held at 20 °C than gels previously held at 4 °C or 40 °C, with a bigger differentiation at lower

concentrations (time lengths not specified) (Schierbaum et al., 1992). Although a thermal hysteresis has been observed in maltodextrin gels through NMR analysis, the bulk properties were not compared nor fully characterized. It was hypothesized that the process of maltodextrin aggregation can vary in type or quantity of associations and the gelling temperature controls the mechanism and resulting gel properties. This article aims to characterize the differences in microstructure created in each of the temperatures and examine any irreversible effects of temperature on the final network and material properties of maltodextrin gels.

2. Materials and Methods:

2.1. Materials

Potato maltodextrin (Paselli SA-2 lot number F3332901) was purchased from Avebe, Netherlands. This maltodextrin has a reported dextrose equivalent (DE) between 2.7-2.9 (Kasapis, Morris, Norton, & Gidley, 1993; Manoj, Kasapis, & Chronakis, 1996) and degree of branching 3.7% (Manoj et al., 1996). Loret et al. (2004a) reported a binomial size distribution of molecular weights centred at 10,290 g/mol and 492,000 g/mol, using size exclusion chromatography. The small MW fraction is known to be the degraded amylose-portions of the starch, and the large MW fraction contains the branched amylopectin regions which were not hydrolysed (Bulpin, et al., 1984; Schierbaum, et al., 1990). Longer chains form associations between aggregated regions, while the shorter chains participate in double helix formation (Loret et al., 2004). The deionised water (DI) used was filtered through a reverse osmosis milli-Q water system. All materials were used with no further purification and no external preservatives or additives were used in the gel systems.

2.2 Preparation of Gels

To prepare gels, maltodextrin was slowly dispersed in heated DI water. The mixture was stirred and heated for 4 hours at 95 °C (+/- 3 °C) to ensure full hydration of the maltodextrin, as indicated by a change in color from white to translucent and results from Chronakis and Kasapis

(1995). Any water lost during heating was added back by matching the initial and final weights. The hot solution of maltodextrin was poured directly into the sampling holder for each test, and all gelation occurred within that pot. Plastic containers were used for deformation properties, aluminium for DSC, and glass for NMR. Samples were sealed or covered to prevent evaporation. To maintain gelling temperatures, samples were placed in thermostated ovens (for 60 °C, 45 °C, and 38 °C) at room temperature (for 22 °C), or in a refrigerator (for 10 °C and 5 °C). All samples were equilibrated to room temperature (22 °C) for 2 hours prior to analysis.

2.3. Large Deformation Properties

The gel strength during compression and fracture was assessed with a texture analyser TA.XT.plus (Stable Micro Systems, UK). This instrument measured the force to move a 6 mm diameter cylindrical probe, with a compression speed of 2 mm/s, into the gel up to a 50% strain. All gels fractured prior to the set 50% strain value, and most fractured between 5 and 15% compressive strain. Cylindrical gels (with a diameter of 20 mm) were cut into pieces of 20 mm height and compressed from the circular face at the centre of the cross section. Measurements were repeated nine times for each sample.

2.4. Differential Scanning Calorimetry

Gel analysis with differential scanning calorimetry (DSC) was performed using a DSC25 (TA Instruments, USA). Samples were prepared by adding the heated solution to a Tzero hermetic pan (TA Instruments, USA) and allowing gelation to completely occur within the sample pan. Prior to analysis, each pan was equilibrated to room temperature. The DSC heated the samples from 20 °C to 120 °C at 5 °C/min with a matching mass of DI water in the reference chamber. Preliminary experiments showed hysteresis in samples that underwent multiple heating treatments, thus all curves are from the first heating cycle. A baseline was constructed by fitting a linear equation to the heat flow before and after the observed peak, and data is reported as the observed signal with a baseline subtraction. The onset temperature was reported as the point of deviation from the

baseline, while peak temperature was calculated at the maximum heat flow. Changes in enthalpy (ΔH) during transitions were determined by integration of the area below the baseline. Changes in entropy (ΔS) were determined utilizing the Gibbs Free Energy equation (ΔG = ΔH – TΔS). Since ΔG is known to be zero at the midpoint of the transition, the change in entropy was calculated through the rearrangement of the equation to $\Delta S = \Delta H/T_{midpoint}$ (Cassanelli, Norton, & Mills, 2018).

2.5. NMR Analysis

Relaxation times (T_2) and rates ($1/T_2$) were measured on a mq20 minispec NMR instrument (Bruker, USA). This instrument operates with a set frequency of 20 mHz. A H20-10-25 AVGX probe and water bath were used to maintain a constant sample temperature of 25 ± 1 °C. A CPMG pulse sequence was used with a pulse separation (tau) of 0.25 ms, 3 dummy echoes, and collection of 615 ms long. Gelation occurred in 8 x 45 mm glass insert tubes (Bruker, USA) covered by cling film. Prior to analysis, all tubes were brought to room temperature (22 °C) before addition to the bottom of a larger 10 mm glass tube (Bruker, USA) and then equilibrated to 25 °C in a heating block.

The relaxation time (T_2) was calculated as the exponent for the decay function, and the relaxation rate was determined by inversing the calculated relaxation time. A manual baseline subtraction was performed prior to fitting the curve. Analysis of the free induction decay suggested solid state signal was present up to 5 ms after the initial pulse, so the exponential function was fitted to the data points from 9 ms to the baseline (400 ms). Each decay function was modelled with a mono-exponential and a bi-exponential decay function and the mean sum of squares of the error was compared using SigmaPlot 12.5 (SYSTAT Software, USA). When the ratio for the bi-exponential function was greater than 5, the more complex function was considered to be a significantly better fit, and two relaxation times were reported. Relaxation curves were also visually assessed for bent appearances to confirm practical differences between relaxation rates determined through the statistical model.

2.6. Transmission Electron Microscopy

Images were obtained on a JEOL JEM-1400 (Tokyo, Japan) transmission electron microscope (TEM). Gels were fixed by placing small pieces in 2.5% aqueous glutaraldehyde for 24 hours followed by 1% osmium tetroxide for 1 hour. Next, samples were dehydrated by two subsequent 15 minute washes in each of 50%, 70%, 90%, 100% alcohol, and propylene oxide. Samples were embedded first in 50% Propylene Oxide / 50% Resin followed by 100% resin and polymerise resin at 60 °C. Thin sections were prepared initially using a microtome and secondly a diamond knife for sections of 50-150 nm. Sections were collected onto Formvar/carbon grids and stained with uranyl acetate.

2.7. Statistical analysis

All measurements were completed in at least triplicate and averages are reported with the single standard deviation. Figures depict the calculated average with error bars showing the standard deviation above and below the average. Comparison of means were conducted by ANOVA analysis followed by an all pairwise multiple comparison test using the Student-Newman-Keuls Method (SigmaPlot 12.5) and significant differences ($p < 0.05$) are shown by unique lettering. Multiple linear regression (MLR) (SigmaPlot 12.5) was used to model individual data points of ΔG, while only the average and standard deviations are shown in Figure 5.

3. Results and Discussion

In this article, maltodextrin gels were evaluated on the bulk level (through large deformation material properties), the molecular level (through DSC and NMR), and the microstructure visualized with TEM. Initially, the impacts of maltodextrin concentration and gelation temperature were evaluated, and subsequently the combination of multiple holding temperatures over various time segments was utilized to study the thermo-reversibility of the network.

3.1. Concentration of Maltodextrin

As is expected with hydrocolloids, an increase in maltodextrin concentration produced gels with an increased gel strength (Figure 1). At 10% maltodextrin (a ratio of 0.11 of solids to water), a gel did not form within 4 days, and the solution remained translucent with some sedimentation. At concentrations of 15% and above (a ratio of 0.18 of solids to water), a white gel formed. At 40% and higher, the gel was firm and crumbly, while 30% and below displayed characteristics of a weak gel. The concentration of polymer in solution clearly dictated the extent of gelation that occurred. Gelation of polymers occurs through association and junction formation between chains, for creation of one continuous network. For maltodextrin, the mechanism of this network formation occurs through two steps: (1) helical association of two strands and (2) aggregation of the double helices into crystalized regions, with longer chains connecting helix aggregates together in a gel (Loret et al., 2004; Reuther et al., 1984; Schierbaum et al., 1990). The crystallization point (as distinguished from the gel point) has been defined as the association between two double- helix chains (4 total chains, with 3 association points) (Loret et al., 2004; Schierbaum et al., 1990). Whereas an increase in viscosity is associated with the formation of 3D structure, cloudiness of gels is attributed to crystallization of the polymer (Loret et al., 2004). Both processes are needed during gel formation to create the necessary structures of a continuous network (Loret et al., 2004). The sedimentation observed in the 10% maltodextrin sample is likely a case of crystallization occurring without gelation. Enough molecules must be present to form helices and begin aggregation, but not enough long chains existed to form a self-supporting network. From 15% and above, chains formed a network with an increasing number of connections and strength. This critical concentration for gelation is higher than most hydrocolloids and is likely due to a high proportion of short or highly branched chains which do not participate in gelation. The relationship between concentration and peak force did not appear to be linear, but instead resembled a second order polynomial (Figure 1), as is commonly observed with biopolymers. Similarly, the storage modulus (G') of maltodextrin has typically been modelled to a non-linear cascade equation (Chronakis, Kasapis, & Richardson, 1996;

Kasapis et al., 1993a; Manoj et al., 1996). The relaxation rate (as determined by NMR) of these gels also followed a similar non- linear trend. Relaxation rates are a measure of the microscopic

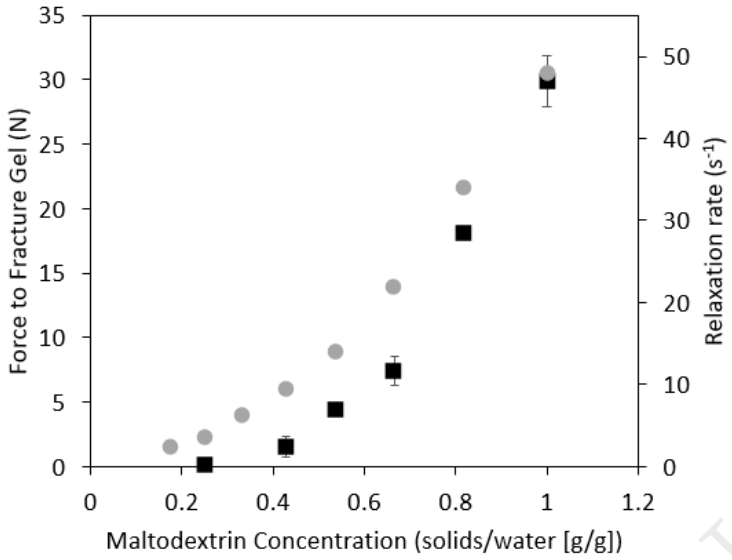

Figure 1. Comparison of the impact of concentration on force to fracture a gel [N] (■) and relaxation rate [s^{-1}] (●) of maltodextrin gels. Error bars represent the average of at least 3 replicates. The force required to fracture a gel was determined by compression and is represented by the average (and standard deviation by error bars) of nine measurement. Determined using NMR, relaxation rate is the exponent for a mono-exponential T_2 decay using the CPMG pulse sequence.

mobility of water, and the correlation between viscosity and relaxation rates has often been observed (German, Blumenfeld, Yuryev, & Tolstoguzov, 1989). Both the gel strength and water mobility suggested that after initial formation of a connecting network, strengthening continued with more polymer (likely through aggregation onto the existing network). Concentration of maltodextrin was shown to be an important factor in gel properties, and the next section will discuss the influence of gelling temperatures.

3.2. Temperature Influence on Gelation

To determine the equilibrium point of gelation, gel strengthening was measured over 14 days for three temperatures. The gel strength increased over the 14 day time range for each of the temperatures (Figure 2). At each time point, the gels formed at 10 °C were significantly stronger than gels at 60 °C and after two days were stronger than the gels at 22 °C. At room temperature, this trend of strengthening (up to 12 days) for a maltodextrin gel has also been reported by Loret et al.

(2004). All three temperatures appeared to reach a practical equilibrium between 4 and 7 days, where the change between days was less than 5 percent. To determine an experimental time point,

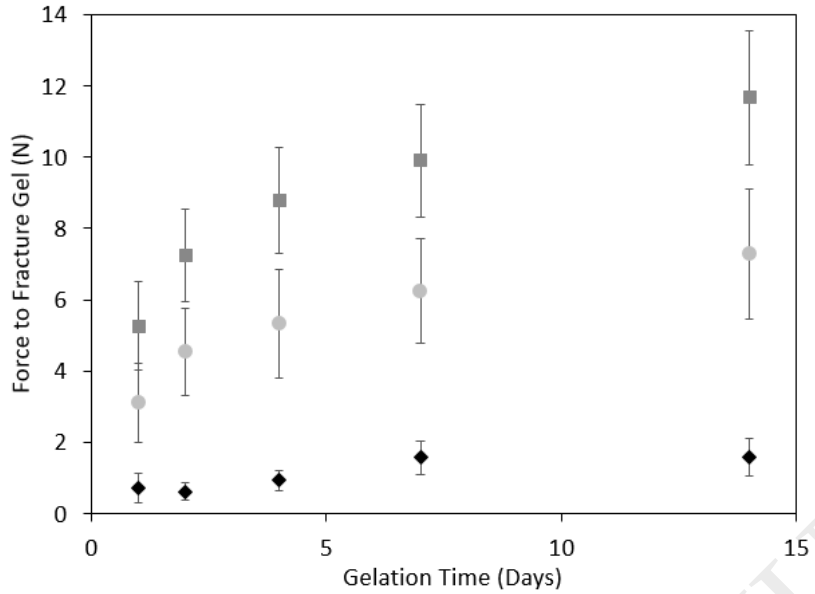

Figure 2. Influence of gelling time and temperature on strength of a 40% maltodextrin gel, after holding at the specified temperature (10 °C ■; 22 °C ●; 60 °C ◆) for the duration of gelation. The force required to fracture a gel was determined by compression and is represented by the average (and standard deviation by error bars) of nine measurement. All measurements took place at room temperature (22 °C) and samples were equilibrated for two hours before analysis.

the curves were fit to a logarithmic function. At four days, there was a change of less than 5% from the previous day (the defined practical equilibrium) and a length of four days was chosen for all future analysis unless otherwise noted. The equilibration observed at each temperature also suggested that temperature impacts the resulting aggregate structure, not just the kinetics of gel formation. After seven days, gels at each of the temperatures have mostly levelled off, without signs of increasing further (Figure 2). This indicates that temperature created a trapped kinetic state of aggregation and structuring. Next, the effect of temperature on gelation was directly compared using various concentrations of maltodextrin, and all were analysed at four days.

3.2.1 Temperature influence on fracture and bulk properties

Gelation at elevated temperatures produced significantly different gel strengths, textures, and microstructures. At higher temperatures, gelation appeared slower and led to weaker gels,

which was consistent at concentrations of 30%, 40%, and 50% (Figure 3). For all concentrations, gelation at 60 °C resulted in a significantly lower gel strength than gelation at 22 °C, 10 °C, or 5 °C. In addition to strength, gels formed at higher temperatures (45 °C and 60 °C) were paste-like, while gels formed at lower temperatures (5 °C and 10 °C) were brittle and crumbly (image inserts in Figure 3 which represent the material after fracture). The strain to fracture the gels were very similar (7-8% for 10 °C but 9-10% for 60 °C) while the mechanisms following fracture demonstrated differences in gel behaviour. The brittle gels broke into pieces and fell away upon fracture (exhibiting a sharp drop in the distance vs. force diagram), while the paste-like gels retained cohesive forces and maintained contact with the probe. Temperature dependence is common for materials measured over a range of temperatures, so all measurements were performed at room temperature and after thermal equilibration, such that variability was reflective only of structural differences. The effect of temperature at the selected concentrations was even shown to be as impactful as concentration. Extremes in the gelling temperature, for the 40% maltodextrin, caused a shift in fracture force from 15 N to 1.7 N (at 5 °C and 60°C respectively). The following comparisons (Figure 3) further highlight the importance of gelling temperature: a 30% solution held at 10 °C formed a stronger gel then 40% held at 60 °C (2.5 N vs. 1.7 N), and a 40% solution held at 5 °C was stronger than a 50% gel formed at

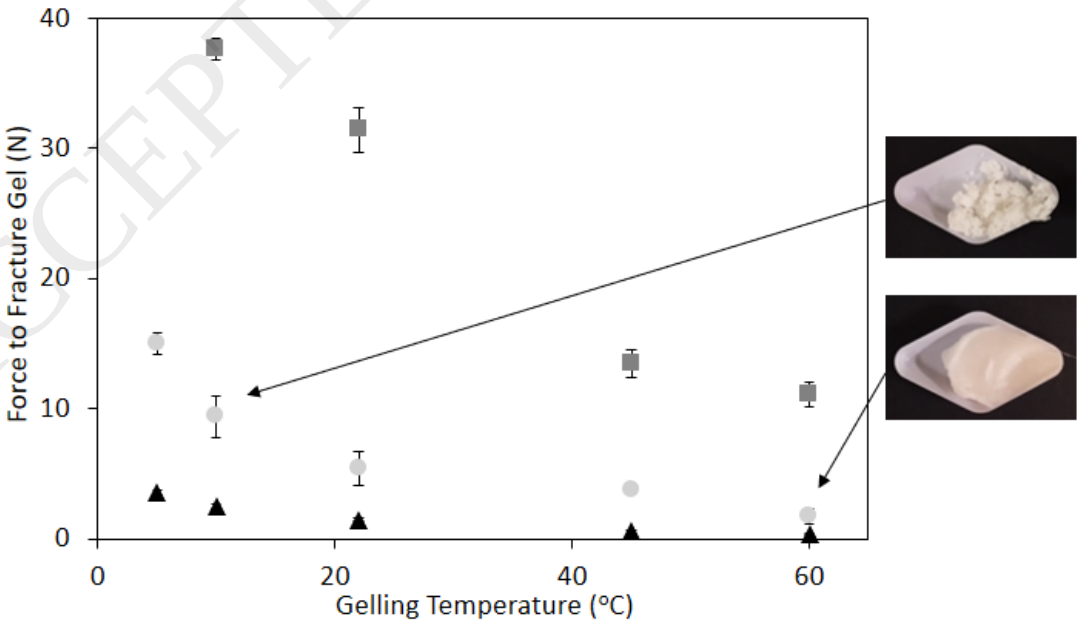

Figure 3. Influence of gelation temperature on gel strength for three concentration levels (50% ■; 40% ●; 30% ▲) of maltodextrin, after holding at the selected temperature for 4 days. Error bars represent the average of at least 3 replicates. The force required to fracture a gel was determined by compression and is represented by the average (and standard deviation by error bars) of nine measurement. All measurements took place at room temperature (22 °C) and samples were equilibrated for two hours before analysis. Image insets display the texture observed after fracture of 40% maltodextrin held at 10 °C and 60 °C.

60 °C (15 N vs. 11 N). These differences in bulk properties presumably originate from different types or extents of network structure, and thus the development of maltodextrin microstructure is temperature dependent. Further tests examined the underlying microstructure to explain these differences.

3.2.2 Temperature influence on water distribution within network

Water mobility within each of the gels was measured through the determination of NMR relaxation rates (the inverse of the relaxation time, T_2). For concentrations of 30% and 40% maltodextrin, there was an observed increase in relaxation rate for structures formed at lower temperatures (Table 1). For each concentration, the sample preparation and measurement temperature of these gels are identical, and thus the changing relaxation rate is clearly an indication of differing microstructures created at the holding temperatures. The faster relaxation rates observed in the samples held at lower temperatures are indicative of less mobile protons. Within gels, faster relaxation rates suggest a stronger and more gelled polymer network with smaller sizes of water pockets (Lillford, Clark, & Jones, 1980; Lillford, 1988). This trend is consistent with the greater fracture force (Section 3.2.1) and greater enthalpy (Section 3.2.3) measured for gels held at lower gelling temperatures. Previous utilization of H-NMR to assess maltodextrin gels also observed a more solid gel at 4 °C than 25 °C for a DE 6 maltodextrin (Schierbaum et al., 1992). However, these experiments preformed measurements at the gelling temperature and thus could not separate the effect of temperature on sample structuring from the holding temperature (Schierbaum et al., 1992). For the current experiments, all measurements took place at 25 °C and thus are true reflections of differences in the aggregate structure. At a concentration of 50%, only gelation at 60 °C produced a different relaxation rate from the other temperatures, which is probably due to the

high solid and low water content. The 50% solid content is approaching the predicted saturation of 71% from the non-freezable water content of 0.4g per 1g of maltodextrin (Radosta & Schierbaum, 1990). As the measured relaxation rate is a weighted average of protons, the high proportion of the bound water appears to be dominating the proton relaxation behaviour.

A few gels exhibited a bi-exponential decay which resulted in two reported relaxation rates. At the temperature extremes (5 °C and 60 °C) two relaxation rates were observed in the 40% sample (at 25.1 s^{-1} and 6.6 s^{-1} for 5 °C and 16.7 s^{-1} and 50.9 for s^{-1} for the 60 °C sample) (Table 1). Two relaxation rates are consistent with a heterogeneous distribution within the gel, and likely from micro-scale syneresis or aggregation of polymer (Lillford et al., 1980). In each case, the rate comprising a majority of the signal follows the expected trend set by the other temperatures, while the second rates fall above and below. The slowest predominant relaxation rate (measured for the sample from 60 °C) also had a minority percentage of very-fast relaxing protons, while the fastest predominant rate had a small proportion of very-slow relaxing protons. These should be reflective of the proton environment of the micro-heterogeneities formed at these extremes. The slow rate (6.6 s^{-1}) is closer to that of pure water and is probably the result of the presence of protons within comparatively large water pockets in the 5 °C sample. Alternatively, the fast relaxation rate (50.9 s^{-1}) of the 60 °C sample originates from a portion of the gel with fast-relaxing protons. It may have been caused by either water molecules within a highly-structured crystalline-like material or polymer protons still in solution, but further NMR analysis would be necessary to confirm the identity. Based on the entropy of the structures, which will be discussed next, the fast relaxation rate present at 60 °C is hypothesized to be from a crystalline-like formation. Consistent with the 40% concentration, the 50% sample held at 60 °C also showed a heterogeneous water distribution. The aggregation structures of maltodextrin were shown to vary with temperature, with micro-heterogeneities observed at both temperature extremes.

3.2.3 Temperature influence on aggregation enthalpy, entropy, and free energy

Impact of temperature on the energy and amount of bonds was explored further with DSC analysis of the samples. Melting curves of maltodextrin gels set at five temperatures are compared in Figure 4 with calculations of melting temperatures, enthalpy, entropy, and free energy changes compiled in Table 2**.** Onset melting temperatures of the networks ranged from 33° to 76° C at a concentration of 40% maltodextrin. Within this temperature range**,** Reuther et al. (1984) confirmed the presence of type-B crystallinity in maltodextrin gels with a melting onset at 56 °C after holding at room temperature (Reuther et al., 1983). From the DSC curves (Figure 4), energies of network formation were examined to determine a mechanism of ordering. Aggregation of maltodextrin chains occurs through hydrogen bonds, and both the enthalpy and entropy of the network were affected by the holding temperature. The higher enthalpy changes (ΔH) measured at lower holding temperatures indicated a greater amount of hydrogen bonds, through more extensive helix formation and aggregation. The lowest enthalpy was observed at high holding temperatures, which was also consistent with the results of a lower gel strength and slower relaxation rates. Although more bonds were formed at low gelling temperatures, a higher melt point was observed in gels formed at higher temperatures. The onset melting temperature was always higher than the temperature used to form the network. Independently, the enthalpy change cannot describe the size of aggregates, but calculation of the entropy leads to an understanding of the size. The shift in melting temperature is a reflection of the increased entropy (ΔS) of the structure, as calculated by the Gibbs Free Energy balance equation ($\Delta G = \Delta H - T\Delta S$) (Cassanelli et al., 2018). Lower entropy structures are reflective of larger aggregate regions with greater compactness and chain lengths. Alternatively, the higher entropy structures formed at low temperatures indicate a more amorphous network with smaller aggregates. DSC analysis allows for the general interpretation that the network formed at high temperature was characterized by higher entropy structures with fewer aggregates, while the low gelling temperature produced a greater number of helices but within less ordered domains.

For comparison of structures of differing entropy and enthalpy, the total energy associated with the networks were compared by calculation of Gibbs Free Energy (ΔG) at each gelling temperature. The relationship between changes in free energy of melting and holding temperature are plotted in Figure 5. A multiple linear regression (MLR) model was fitted using parameters of temperature (in °C) and concentration (as a percent) yielding the equation ΔG = 1.31 - 0.034*Temperature + 0.023*Concentration with an R^2 of 0.87. The calculated free energy changes

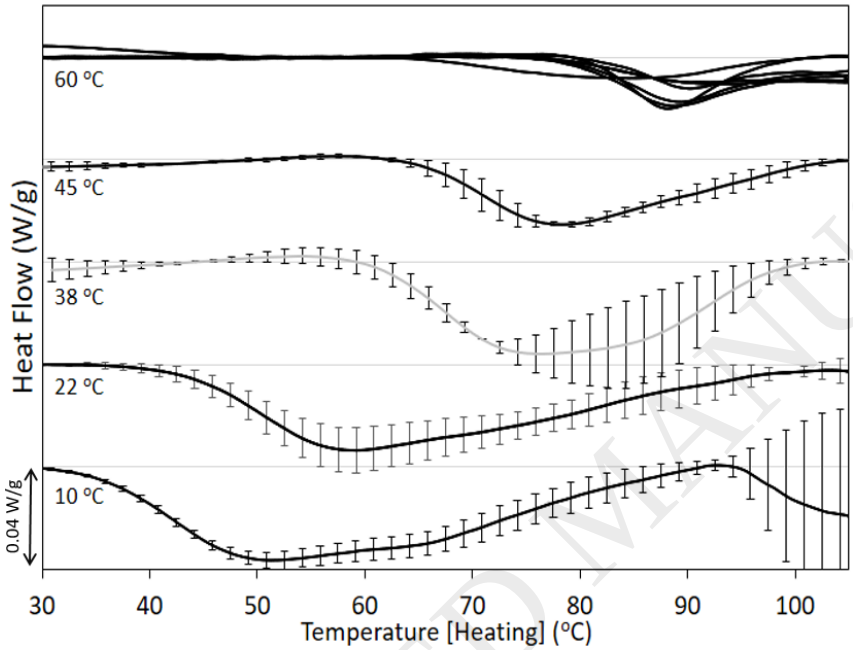

Figure 4. Melting DSC endotherm of 40% maltodextrin gels set for four days at the indicated temperature. A heating rate of 5 °C/min was utilized with a reference cell of water. Error bars represent the standard deviation of three replicates.

are overlaid with the MLR fit for concentration of 40% (●) and 30 % (▲) in Figure 5. Extending protein folding-unfolding theory to maltodextrin gelation suggests the zero-intercepts of the free energy represent the chemical equilibrium between aggregation and remaining in solution (Santoro & Bolen, 1992). Extrapolation to a zero free energy value resulted in critical aggregation temperatures of 66 °C and 59 °C for 40% and 30% respectively. At 60 °C, no gel network was detectable by DSC for the 30% maltodextrin sample. The zero enthalpy temperature of 30% falls below 60 °C, and as would be predicted, no bonds were detectable in these samples. High variability seen in replicates of Figure 4 for 60 °C further suggested these bonds are likely near the critical

temperature for formation of helix and aggregates so the number in each replicate is highly variable. These critical temperatures represent the chemical equilibrium shifting from ordered and aggregated chains to non-aggregated random coils. At low temperatures, the enthalpy of helix

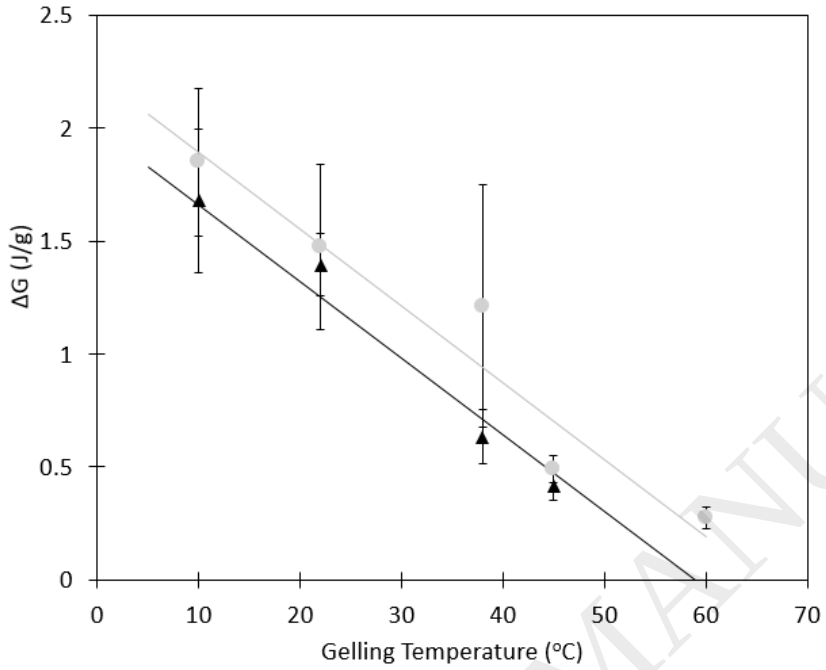

Figure 5. Holding temperature influence on Free Energy (Δ G) calculated from DSC thermographs. A multiple linear regression (MLR) was fitted to concentration [40% (●) and 30 % (▲)] and holding temperature. The resulting equation was ΔG = 1.31 - 0.034*Temperature + 0.023*Concentration with an R^2 of 0.87.

formation leads to the most network development and the greatest energy potential. Increasing temperature progressively favors the increasing energy contribution from entropy of polymers within the random coil form. This trend is not expected to hold below the temperature of 0 °C due to the complexity of water freezing in competition with chain aggregation.

Compared to the sharp peaks typical of many melting hydrocolloids, the thermographs of maltodextrin showed the gels melted over a relatively wide temperature range. The most notable range was observed at the low gelling temperatures, with the gel formed at 10 °C melting from 30 °C to 90 °C (Figure 4). A wide melting peak is also consistent with previous DSC analysis of maltodextrin gels (Schierbaum et al., 1992). The broad melting temperature range, indicative of heterogeneity in

structure, is consistent with the gelation mechanism of aggregation and the wide dispersion of chain lengths of a maltodextrin product. Chain length variability and differences in ordering mechanisms are then the likely cause of this wide range. This range is likely also a factor in the observed difference in aggregation at each of the temperatures.

The progressive increase in melting temperature (and subsequent decreasing of entropy) suggests a shifting equilibrium of aggregation with holding temperature. The larger number of bonds and higher entropy is proposed to be caused by the effect of temperature on helix-coil transition (solubility) of the maltodextrin chains. Gelation occurs between molecules in the more-structured helix form. Low temperatures favored the aggregation of amylose chains (German, Blumenfeld, Guenin, Yuryev, & Tolstoguzov, 1992), likely through a greater proportion of chains in the helix form. However, increased temperature decreases the proportion of chains in the helix versus coil state (Moates, Noel, Parker, & Ring, 1997). As insolubility of the helix form is a driver for gelation, a greater proportion of chains in the coil form at elevated temperatures would decrease the extent of gelation. This is consistent with the observed decreasing enthalpy. Based on the higher melting temperature for gelation at 45 °C and 60 °C, the shorter chains appear to not have participated in gelation. These smaller polymers are proposed to be in the random coil state at these temperatures and subsequently stay within the aqueous phase. Instead, the longer chains which are in the helix state contributed to network formation. Participation by the larger molecular weight fraction at higher temperatures is consistent with the lower entropy measured for these structures, previously described as consisting of larger and more ordered aggregates of longer chain lengths. In summary, the smaller enthalpy and entropy at high temperatures was proposed to be a reflection of decreasing contribution of the smaller molecular weight fraction to the aggregation network.

3.2.4 Temperature influence on aggregate structure

To visualize the aggregation structures, transmission electron microscopy (TEM) images were obtained. The first step of sample preparation consisted of adding small sections of sample to

an aqueous glutaraldehyde solution. Thus, the images represent the non-dissolvable content of each sample as some material was expect to disperse in the solution. From the observed network, the size of crystals was largest in the 60 °C sample (2-4 µm) compared to 22 °C (2 µm) or 10°C sample (1-2 µm) (Figure 6). A greater crystallinity was also seen in the 60 °C than either the 22 °C or 10 °C,

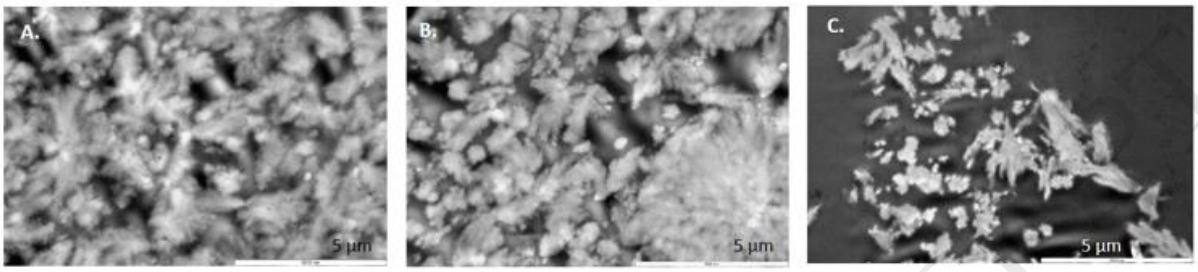

Figure 6. TEM images of maltodextrin networks (at 40%) held for four days at (A)10 ^{o}C, (B) 22 ^{o}C and (C) 60 ^{o}C. Each image is 12 x 8 µm.

indicated by more blurry images at 10 °C caused by diffusion of electrons passing through amorphous regions. These images support the previous claims of larger aggregate zones and a more crystalline-like network when held at 60 °C. The presence of larger crystalline regions is also consistent with the small proportion of fast-relaxing protons only observed for the sample held at 60 °C. Although the gels have equilibrated to the selected temperature, moving the gel to a different temperature may modify the equilibrium point. To examine this concept, the thermal reversibility of the structure was analysed to determine if these bonds remained after moving to a different temperature.

3.3. Thermal Hysteresis of Gel Network

In the previous section, the gelling temperature was shown to impact structure formation. A constant temperature created a gel network approaching an apparent equilibrium. Next, hysteresis of the gelation network was examined by holding samples at multiple temperatures to assess whether these structures were thermally reversible. After an initial gelation period of 4 days, samples were moved to a second gelation temperature for 2 days (Figure 7A) and 6 days (Figure 7B). Consistent with work reported in the previous section, all samples were equilibrated to room temperature (22 °C) for two hours prior to analysis. Points along the dotted grey line represent the

control samples which were kept at the same temperature during both gelling periods. Deviation from this control line show the influence of the second temperature. A lower (colder) second gelling temperature generally increased the gel strength, while a higher temperate decreased the strength

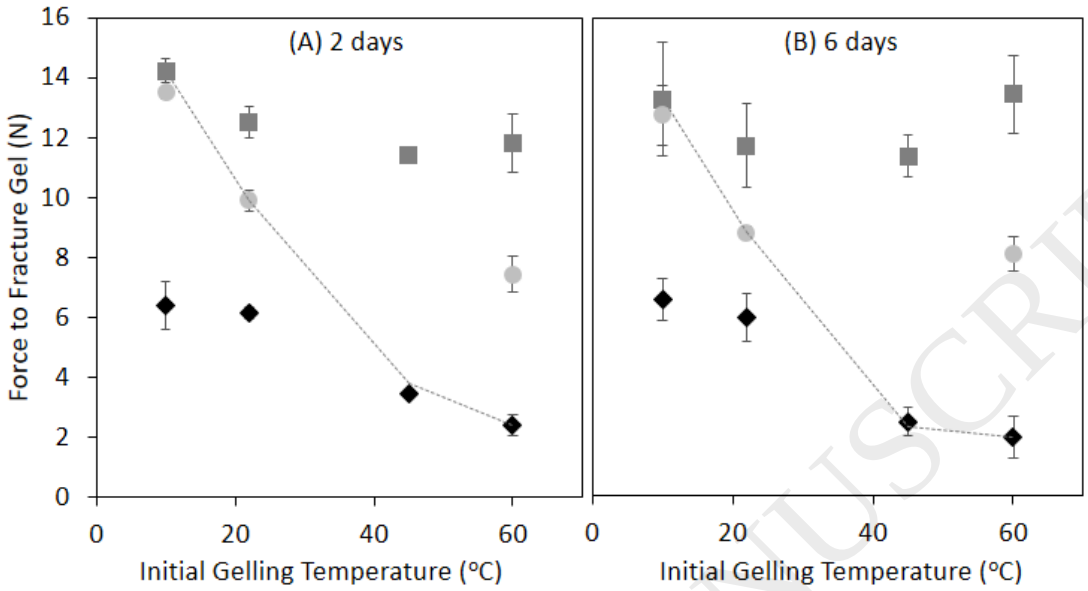

Figure 7. Reversibility of gel structure for a 40% maltodextrin, after holding at the initial temperature for 4 days and the secondary temperature (10 °C ■ ; 22 °C ●; 60 °C ◆) for (A) 2 days and (B) 6 days . The dotted line represents the control samples which were maintained at a constant temperature.

(Figure 7). The strength of gels held at a second temperature of 10 °C and 22 °C were higher than the control gel at 60 °C (peak forces of 13 N, 8 N, and 2 N respectively). Following a second holding period of 6 days at 10 °C, none of the samples initially held at other temperatures were significantly different in gel strength than a gel continuously held at 10 °C. However, a second gelling temperature of 60 °C showed hysteresis. A gel formed at 10 °C or 22 °C did not (after 2 or 6 days) adjust to the strength of a gel at 60 °C. Some of the network formed at 10 °C or 22 °C is preserved, even if the temperature is changed, indicating the irreversibility of some associations. To further analyse this partially reversible network, the relaxation rates of water within the gel were compared using NMR.

In agreement with analysis of the fracture properties, the water relaxation also displayed a hysteresis when subjected to multiple temperature holds. For all four of the initial gelling

temperatures, a second hold at 10 °C formed a gel with the fastest relaxation rate and 60 °C at the slowest relaxation rate (Table S1). Moving to a cooler second temperature increased the solidity of the network (faster relaxation rate), while a warmer second temperature formed a more mobile network. Interestingly, gels initially held at 60 °C all showed two relaxation times, consistent with a heterogeneous material. As previously discussed, the appearance of a minor portion of protons relaxing with a faster rate was predicted to be indicative of crystalline-like regions. The presence of highly-ordered structures in all samples that initially gelled at 60 °C suggests an irreversible formation at this temperature. Previously described as highly ordered aggregation regions, these seem to be of high stability and only formed at 60 °C. Shifts over time and at other temperatures could be using these junction zones as a seed point for further growth. Comparing the magnitude of the second relaxation rates, the ordering is probably a reflection of the average size of the regions. Interestingly, the fracture strength of these three samples did not show signs of hysteresis, but the relaxation rates indicate the microstructure is different. Further analysis of the microstructure investigated the bond energies of the networks using DSC.

The network remaining after multiple temperature holds was investigated to detect any type of irreversible structures. As indicated previously (section 3.2), the associations formed at 10 °C have a melting onset of 30 - 35 °C and peak of 50 - 55 °C, while the network formed at 60 °C has a melting onset of 70 - 80 °C with a peak of 90 - 95 °C (Figure 4). When gels were held at two temperatures, melting peaks were observed at temperatures reflective of a combination of each gelling condition (Figure S1 and Table 3). Bimodal DSC melting peaks have also been observed in gelatin gels, and two types of structure (formed at each of the holding temperatures) was similarly proposed (Busnel, Clegg, & Morris, 1988). Based on corresponding enthalpy values (Table 3), the amount of gel structuring was more reflective of the secondary gelling temperature than the initial temperature. Moving a gel set at 10 °C to an environment at 60 °C, only 2 J/g of bond energy remained at the expected 10 °C position, while 8 J/g of new bonds were formed reflective of the secondary gelling temperature (60 °C). Similarly, with an initial gelling temperature of 60 °C and secondary hold at 10

°C, 1 J/g of bond energy (of the 3 J/g) remained at the expected 60 °C position, while 9 J/g were formed at the 10 °C location. For each of these switches, the enthalpy values created in the second holding temperature were also different than a single temperature hold. With an initial hold of

Table 3. Calculated melting onset temperatures, enthalpy of melting values, and entropy from DSC curves after holding at the initial temperature for 4 days and the secondary temperature for 6 days. Letters signify samples that are significantly different means through all pairwise comparisons (Student-Newman-Keuls Method).

10 °C, more associations formed at the 60 °C location (8 J/g versus 3 J/g without another temperature hold). Thus, the bonds formed during the 10 °C hold enhanced aggregation at the second temperature hold of 60 °C. This disparity is likely due to a seeding effect of the high entropy bonds formed at the first temperature that initiated lower entropy associations. At 10 °C, there were minimal bonds melting near 90 °C, so any residual bonding from the first hold does not account for the difference. Previously, the low entropy bonds formed at 60 °C were proposed to be near the critical gelling point due to the high variability and low enthalpy (section 3.2). This apparent influence of seeding to increase gelation supports the previous hypothesis that gelation at 60 °C is near the edge of stability. Examining the opposite transition, from 60 °C to 10 °C, there was alternatively a decrease in the number of bonds formed at the second gelling temperature (8 J/g versus 14 J/g without another temperature hold). In this transition, the bonds formed at 60 °C appeared to inhibit aggregation and bond formation at the second holding temperature. The low entropy bonds characteristic of gelation at 60 °C were proposed to lead to larger junction zones, and it may be these bulky structures sterically inhibit high entropy bonds. Some of the structuring formed at 60 °C (with a melting point between 80 - 95 °C) breaks apart while holding at a second temperature, as seen in the decreased in the enthalpy from 3 J/g to 1 J/g (switching to 10 °C). The sample was never at a temperature high enough to melt, so the low entropy configuration must not be stable at 10 °C. A minor proportion of the maltodextrin aggregation shows thermal irreversibility, although the resulting network is more reflective of the ending thermal influence.

4. Conclusion:

Temperature was shown to impact the size of chains participating in the helix formation and the organization of helices during network development, and thus the hypothesis was supported. Previous work had focused on temperature's effect on gelation speeds, but the novelty of this work examined the impacts on the near-equilibrated gel microstructure and fracture properties. Importantly, all analysis was completed at identical temperatures, so results are a true reflection of the underlying structure differences formed at the gelling temperatures. Gels formed at lower temperatures (10 °C) were stronger and more brittle which corresponded to a higher entropy network with a greater number of aggregates. Higher holding temperatures (up to 60 °C) resulted in less network formation and lower entropy creating the appearance of a weak gel. An exploration of the spontaneity of aggregation through shifting entropic and enthalpic contributions demonstrated the importance of temperature in controlling molecular ordering. Holding temperature was proposed to influence the amount of smaller molecular weight chains participating in aggregating by shifting from the helix to coil form at higher temperatures. The low entropy structure formed at high temperatures is of particular interest as it could prove to impart novel digestion properties to the maltodextrin gels. This demonstrated control of gelation mechanism through temperature allows for selection of ideal properties to use in food applications such as mixed gel preparation.

Acknowledgements

This research was partially funded by the Engineering and Physical Sciences Research Council [grant number EP/K030957/1], the EPSRC Centre for Innovative Manufacturing in Food. Additional thanks to Dr Peter Lillford for assistance with NMR analysis and Dr Rob Child for discussion.

References

Brown,C., Foster T. J., Norton I. T., & Underdown J. (1995). Influence of shear on the microstructure of mixed biopolymer systems. *Biopolymer Mixtures* , 65-83.

Bulpin,P. V., Cutler A. N., & Dea I. (1984). Thermally-reversible gels from low DE maltodextrins. *Gums and Stabilizers for the Food Industry 2*, 475-484.

Busnel, J. P., Clegg, S. M., & Morris, E. R. (1988). Melting behaviour of gelatin gels: origin and control. In G.O. Phillips, D. J. Wedlock & P. A. Williams (Ed.). *Gums and Stabilisers for the Food Industry 4, Eds.*(pp. 105-115). Oxford: IRL.

Butler, M. F. & Heppenstall-Butler, M. (2003). Phase separation in gelatin/dextran and gelatin/maltodextrin mixtures. *Food Hydrocolloids 17*, 815-830.

Cain, F. W., Clark, A. H., Dunphy, P. J., Jones, M. G., Norton, I. T., & Ross-Murphy, S. B. (1990). U.S. Patent No. 4,956,193. Edible plastic dispersion.

Cassanelli,M., Norton I., & Mills T. (2018). Interaction of Mannitol and Sucrose with Gellan Gum in Freeze-Dried Gel Systems. *Food Biophysics* , 1-12.

Chronakis,I. S. (1998). On the molecular characteristics, compositional properties, and structural-functional mechanisms of maltodextrins: a review. *Critical Reviews in Food Science and Nutrition 38*, 599-637.

Chronakis, I. S. & Kasapis, S. (1995). Preparation and Analysis of Water Continuous Very Low Fat Spreads. *LWT - Food Science and Technology 28*, 488-494.

Chronakis,I. S., Kasapis S., & Richardson R. K. (1996). Small deformation rheological properties of maltodextrin—milk protein systems. *Carbohydrate Polymers 29*, 137-148.

German,M. L., Blumenfeld A. L., Guenin Y. V., Yuryev V. P., & Tolstoguzov V. B. (1992). Structure formation in systems containing amylose, amylopectin, and their mixtures. *Carbohydrate Polymers 18*, 27-34.

German,M. L., Blumenfeld A. L., Yuryev V. P., & Tolstoguzov V. B. (1989). An NMR study of structure formation in maltodextrin systems. *Carbohydrate Polymers 11*, 139-146.

Kasapis,S., Morris E. R., Norton I. T., & Brown C. R. T. (1993). Phase equilibria and gelation in gelatin/maltodextrin systems - Part III: Phase separation in mixed gels. *Carbohydrate Polymers 21*, 261-268.

Kasapis, S., Morris, E. R., Norton, I. T., & Clark, A. H. (1993a). Phase equilibria and gelation in gelatin/maltodextrin systems — Part I: gelation of individual components. *Carbohydrate Polymers 21*, 243-248.

Kasapis, S., Morris, E. R., Norton, I. T., & Clark, A. H. (1993b). Phase equilibria and gelation in gelatin/maltodextrin systems — Part IV: composition-dependence of mixed-gel moduli. *Carbohydrate Polymers 21*, 269-276.

Kasapis,S., Morris E. R., Norton I. T., & Gidley M. J. (1993). Phase equilibria and gelation in gelatin/maltodextrin systems - Part II: Polymer incompatibility in solution. *Carbohydrate Polymers 21*, 249-259.

Lillford, P. J. (1988). The polymer/water relationship--its importance for food structure. In JMV Blanshard & JR Mitchell (Eds.). *Food Structure: Its Creation and Evaluation* (pp. 75-92). : London: Butterworths, 1988.

Lillford, P. J., Clark, A. H., & Jones, D. V. (1980). Distribution of water in heterogeneous food and model systems. In Anonymous *Water in Polymers* (Vol. 127, pp. 177-195). : ACS Symposium Series.

Loret, C. L., Frith, W. J., & Fryer, P. J. (2006). Microstructures Designed to Control the Mechanical Properties of Mixed Biopolymer Gels. In O. Phillips Glyn & P. A. Williams (Eds.). *Gums and Stabilisers for the Food Industry 13* (pp. 185-192). : Royal Society of Chemistry.

Loret, C. L., Frith, W. J., & Fryer, P. J. (2004). Mechanical properties of maltodextrin gels: Small and large deformation. In G. O. Phillips & P. A. Williams (Eds.). *Gums and Stabilisers for the Food Industry 12* (pp. 116-123). : The Royal Society of Chemistry.

Loret, C. L., Meunier, V., Frith, W. J., & Fryer, P. J. (2004). Rheological characterisation of the gelation behaviour of maltodextrin aqueous solutions. *Carbohydrate Polymers 57*, 153-163.

Lorn,N. & Hermansson A. (2000). Phase separation and gel formation in kinetically trapped gelatin/maltodextrin gels. *International Journal of Biological Macromolecules 27*, 249-262.

Lundin, L., Norton, I. T., Foster, T. J., Williams, M., Hermansson, A. M., & Bergstrom, E. (2000). Phase Separation in Mixed Biopolymer Systems. In Peter A. Williams, Glyn O Phillips (Ed.). *Food Colloids, Biopolymers and Materials 10* (pp. 1). : Royal Society of Chemistry.

Manoj,P., Kasapis S., & Chronakis I. S. (1996). Gelation and phase separation in maltodextrin-caseinate systems. *Food Hydrocolloids 10*, 407-420.

Moates,G. K., Noel T. R., Parker R., & Ring S. G. (1997). The effect of chain length and solvent interactions on the dissolution of the B-type crystalline polymorph of amylose in water. *Carbohydrate Research 298*, 327-333.

Nickerson,M. T., Farnworth R., Wagar E., Hodge S. M., Rousseau D., & Paulson A. T. (2006). Some physical and microstructural properties of genipin-crosslinked gelatin–maltodextrin hydrogels. *International Journal of Biological Macromolecules 38*, 40-44.

Normand,V., Plucknett K. P., Pomfret S. J., Ferdinando D., & Norton I. T. (2001). Large deformation mechanical behavior of gelatin–maltodextrin composite gels. *Journal of Applied Polymer Science 82*, 124-135.

Picout, D. R., Richardson, R. K., & Morris, E. R. (2000). Co-gelation of calcium pectinate with potato maltodextrin. Part 1. Network formation on cooling. *Carbohydrate Polymers 43*, 133-141.

Radosta,S. & Schierbaum F. (1990). Polymer-Water Interaction of Maltodextrins. Part III: Non-freezable Water in Maltodextrin Solutions and Gels. *Starch-Stärke 42*, 142-147.

Reuther,F., Damaschun G., Gernat C., Schierbaum F., Kettlitz B., Radosta S., & Nothnagel A. (1984). Molecular gelation mechanism of maltodextrins investigated by wide-angle X-ray scattering. *Colloid & Polymer Science 262*, 643-647.

Reuther,F., Plietz P., Damaschun G., Pürschel H., Kröber R., & Schierbaum F. (1983). Structure of maltodextrin gels—a small angle X-ray scattering study. *Colloid and Polymer Science 261*, 271-276.

Santoro,M. M. & Bolen D. W. (1992). A test of the linear extrapolation of unfolding free energy changes over an extended denaturant concentration range. *Biochemistry 31*, 4901-4907.

Schierbaum,F., Radosta S., Vorwerg W., Yuriev V. P., Braudo E. E., & German M. L. (1992). Formation of thermally reversible maltodextrin gels as revealed by low resolution H-NMR. *Carbohydrate Polymers 18*, 155-163.

Schierbaum,F., Reuther F., Braudo E. E., Plashchina I. G., & Tolstoguzov V. B. (1990). Thermodynamic parameters of the junction zones in thermoreversible maltodextrin gels. *Carbohydrate Polymers 12*, 245-253.

Wesdorp, L. H., Madsen, R. A., Norton, I. T., & Brown, C. R. (1995). U.S. Patent No. 5,464,645. Process of making a water continuous dispersion with more than 50% dispersed phase and products thereof.

Table 1. Measured relaxation rates at 25 °C for 30 %, 40%, and 50% maltodextrin gels, after holding at the indicated temperature for 4 days.

Maltodextrin Concentration	Gelation Temperature (4 days)	$1/T_2$ (1^{st}) Relaxation Rate (s^{-1})	$1/T_2$ (1^{st}) Amplitude %	$1/T_2$ (2^{nd}) Relaxation Rate (s^{-1})	$1/T_2$ (2^{nd}) Amplitude %
50 %	60 °C	51.9 ± 5.4	82 %	37.0 ± 2.3	18 %
	45 °C	44.3 ± 0.3	100 %		
	22 °C	45.1 ± 0.5	100 %		
	10 °C	45.3 ± 0.9	100 %		
	5 °C	44.9 ± 0.0	100 %		
40 %	60 °C	16.7 ± 0.7	83 %	50.9 ± 3.3	17 %
	45 °C	16.6 ± 0.2	100 %		
	22 °C	20.6 ± 0.3	100 %		
	10 °C	22.3 ± 0.1	100 %		
	5 °C	25.1 ± 0.1	98 %	6.6 ± 0.5	2 %
30 %	60 °C	7.2 ± 0.5	100 %		
	45 °C	7.7 ± 0.3	100 %		
	22 °C	10.5 ± 0.5	100 %		
	10 °C	12.0 ± 0.5	100 %		

Table 2. Calculated melting temperatures, enthalpy, and entropy values from DSC heating endotherms of maltodextrin gels set for four days at the indicated temperature. A heating rate of 5 °C/min was utilized with a reference cell of water. Averages are reported with one standard deviation (of three replicates except 40% at 60 °C which is the average of 7 replicates).

Maltodextrin Concen-tration	Gelation Temperature	Calculations from DSC heating endotherms				
		Onset (°C)	Midpoint (°C)	ΔH (J/g)	ΔS (mJ/g·K)	ΔG (J/g)
40 %	60 °C	76.0 ± 4.3	89.0 ± 1.6	3.4 ± 0.6 ^{A}	9.5 ± 1.5 ^{A}	0.27 ± 0.05 ^{A}
	45 °C	64.3 ± 2.9	77.7 ± 1.5	5.3 ± 0.9 ^{A}	15.1 ± 2.5 ^{A}	0.49 ± 0.06 ^{A}
	38 °C	58.0 ± 2.0	77.3 ± 5.1	10.4 ± 3.1 ^{B}	29.6 ± 8.2 ^{B}	1.2 ± 0.5 ^{B}
	22 °C	42.7 ± 3.2	59.3 ± 0.58	13.1 ± 3.3 ^{B}	39.5 ± 9.8 ^{BC}	1.5 ± 0.4 ^{BC}
	10 °C	33.0 ± 2.6	51.3 ± 0.58	14.5 ± 2.7 ^{B}	44.8 ± 8.0 ^{C}	1.8 ± 0.3 ^{C}
30 %	60 °C	- **	- **	- **	N/A	N/A
	45 °C	66.3 ± 2.1	81.3 ± 1.5	4.0 ± 0.6 ^{A}	11.4 ± 1.7 ^{A}	0.41 ± 0.06 ^{A}
	38 °C	59.0 ± 3.6	79.7 ± 0.6	5.4 ± 0.9 ^{A}	15.2 ± 2.6 ^{A}	0.63 ± 0.1 ^{A}
	22 °C	39.0 ± 1.0	63.0 ± 2.6	11.4 ± 0.5 ^{B}	34.0 ± 1.2 ^{B}	1.4 ± 0.1 ^{B}
	10 °C	37.0 ± 2.6	53.0 ± 1.0	12.8 ± 2.7 ^{B}	39.1 ± 8.3 ^{B}	1.7 ± 0.2 ^{B}

**Peaks could not be resolved from baseline

Table 3. Calculated melting onset temperatures, enthalpy of 467 melting values, and entropy from DSC curves after holding at the initial temperature for 4 days and the secondary temperature for 6 days. Letters signify samples that are significantly different means through all pairwise comparisons (Student-Newman-Keuls Method).

				1st Peak			2nd Peak		
1st Temp (4 days)	2nd Temp (6 days)	Total ΔH (J/g)	Total ΔG at 22 (J/g)	Midpoint (°C)	ΔH (J/g)	ΔS (mJ/g·K)	Midpoint (°C)	ΔH (J/g)	ΔS (mJ/g·K)
60 °C	60 °C	2.9 ± 0.3^{A}	0.56 ± 0.04^{A}	- **	- **	- **	94.0 ± 1.4	2.9 ± 0.3	7.8 ± 0.7
60 °C	10 °C	9.2 ± 0.9^{B}	0.99 ± 0.15^{B}	53.3 ± 0.6	7.6 ± 0.8	23.3 ± 2.6	91.3 ± 3.2	1.5 ± 0.9	4.1 ± 2.4
45 °C	10 °C	11.3 ± 1.3^{B}	1.5 ± 0.5^{C}	- *	-*	- *	- *	-*	-*
22 °C	60 °C	10.1 ± 1.3^{B}	1.6 ± 0.2^{C}	49.8 ± 1.0	2.3 ± 0.4	7.0 ± 1.3	88.3 ± 0.5	7.8 ± 1.0	21.6 ± 2.7
10 °C	60 °C	10.1 ± 1.2^{B}	1.6 ± 0.2^{C}	49.8 ± 2.1	2.0 ± 0.6	6.2 ± 1.7	86.5 ± 0.6	8.1 ± 0.7	22.4 ± 2.0
10 °C	10 °C	13.9 ± 0.1^{C}	1.3 ± 0.02^{BC}	52.5 ± 0.7	13.9 ± 0.1	42.8 ± 0.4	- **	- **	- **

*Peaks could not be resolved from each other

**Peaks could not be resolved from baseline

Table S1. Water relaxation rates, measured at 25 °C, for 40% maltodextrin gels, after holding at the initial temperature for 4 days and the secondary temperature for 6 days.

1st Gelation Temperature (4 days)	2nd Gelation Temperature (6 days)	T_2 (1st)		T_2 (2nd)	
		Relaxation Rate (s^{-1})	Amplitude %	Relaxation Rate (s^{-1})	Amplitude %
10 °C	10 °C	24.7 ± 0.1	96 %	10.7 ± 0.1	4 %
	22 °C	23.2 ± 0.0	100 %		
	60 °C	19.4 ± 0.1	100 %		
22 °C	10 °C	23.1 ± 0.0	100 %		
	22 °C	21.7 ± 0.1	100 %		
	60 °C	18.9 ± 0.1	100 %		
45 °C	10 °C	25.6 ± 0.4	94 %	13.9 ± 2.9	6 %
	45 °C	17.9 ± 0.2	100 %		
	60 °C	17.0 ± 0.1	100 %		
60 °C	10 °C	29.4 ± 0.7	70 %	21.1 ± 0.7	30 %
	22 °C	22.2 ± 0.2	74 %	34.6 ± 0.7	26 %
	60 °C	20.0 ± 0.1	89 %	54.0 ± 3.6	11 %